ON THE BRIGHTNESS AND WAITING-TIME DISTRIBUTIONS OF A TYPE III RADIO

STORM OBSERVED BY STEREO/WAVES

ON THE BRIGHTNESS AND WAITING-TIME DISTRIBUTIONS OF A TYPE III RADIO STORM OBSERVED BY STEREO/WAVES

J. P. Eastwood[1], M. S. Wheatland[2], H. S. Hudson[1], S. Krucker[1], S. D. Bale[1,3], M. Maksimovic[4], K. Goetz[5], and J.-L. Bougeret[4]
[1] Space Sciences Laboratory, University of California, Berkeley, CA 94720, USA; eastwood@ssl.berkeley.edu
[2] Sydney Institute for Astronomy, School of Physics, The University of Sydney, NSW 2006, Australia
[3] Department of Physics, University of California, Berkeley, CA 94720, USA
[4] LESIA, Observatoire de Paris, F-92195 Meudon, France
[5] School of Physics and Astronomy, University of Minnesota, Minneapolis, MN 55455, USA

ABSTRACT

Type III solar radio storms, observed at frequencies below ∼16 MHz by space-borne radio experiments, correspond to the quasi-continuous, bursty emission of electron beams onto open field lines above active regions. The mechanisms by which a storm can persist in some cases for more than a solar rotation whilst exhibiting considerable radio activity are poorly understood. To address this issue, the statistical properties of a type III storm observed by the STEREO/WAVES radio experiment are presented, examining both the brightness distribution and (for the first time) the waiting-time distribution (WTD). Single power-law behavior is observed in the number distribution as a function of brightness; the power-law index is ∼2.1 and is largely independent of frequency. The WTD is found to be consistent with a piecewise-constant Poisson process. This indicates that during the storm individual type III bursts occur independently and suggests that the storm dynamics are consistent with avalanche-type behavior in the underlying active region.

Key words: methods: statistical – Sun: activity – Sun: corona – Sun: radio radiation

1. INTRODUCTION

Type III solar radio storms consist of many individual type III radio bursts produced quasi-continuously over several days (Fainberg & Stone 1970a, 1970b, 1971). Such storms can persist for long intervals—they have been observed for up to half a solar rotation, and in some cases over a whole rotation (Fainberg & Stone 1970a). It has been shown that they are associated with both active regions and metric type I storms (Kayser et al. 1987; Gopalswamy 2004). The type III storm emission is produced by electron beams on open field lines (Bougeret et al. 1984a, 1984b), and so type III storm activity may shed light on the dynamics of the open/closed field line boundaries associated with the underlying active region. The dynamics of type III storms are still not well understood, particularly the mechanisms by which they are able to persist for such long times whilst at the same time generating considerable numbers of radio bursts. Furthermore, type III storms have also been observed as precursors to coronal mass ejections (Reiner et al. 2001), and so a better understanding of their properties may help to elucidate the dynamics of active regions prior to eruptive events.

One important statistical property is the distribution of power S in the individual bursts. In their initial type III storm study, Fainberg & Stone (1970a) noted that there were more faint bursts than bright ones. More recently, Morioka et al. (2007) studied the statistics of type III bursts using Geotail (24 Hz–800 kHz) and Akebono (20 kHz–5 MHz) radio data. Using observations covering four Bartels rotations and containing both ordinary type III emission and intervals of type III storm activity, they found that the overall occurrence of type III bursts followed a double power law; for example, at a frequency of 860 kHz and below an intensity of $\sim 10^{-15}$ V^2 m^2 Hz^{-1} ($\sim 2.7 \times 10^{-18}$ W m^{-2} Hz^{-1}), the number distribution (simply the number of bursts at a given brightness) followed a $S^{-3.6}$ power law, whereas above this limit, a $S^{-0.52}$ power law was

observed. Morioka et al. (2007) named the lower flux distribution "micro-type III bursts," and concluded that although they were associated with the same active regions as the "ordinary" type III bursts, they were produced by independent, coexisting processes. This is consistent with the association of the type III storms with meter-wave type I "noise storms," which do not have the close association with flares that characterizes ordinary type III bursts (e.g., Gopalswamy 2004). In comparison, Fitzenreiter et al. (1976) found in a study of ordinary type III bursts observed over a period of three months that the number/unit flux density fell off with increasing flux following a $S^{-\beta}$ power law with β varying from 1.33 at 110 kHz to 1.69 at 4.9 MHz. This in fact appears compatible with the Morioka et al. (2007) study, since a $S^{-1.69}$ power law in the number/unit flux density corresponds to a $S^{-0.69}$ power law in the number distribution. For comparison, at higher frequencies (164 MHz, 237 MHz, and 327 MHz), the number distribution of type I bursts in radio noise storms has been found to follow a similarly steep S^{-3} power law (Mercier & Trottet 1997).

A second statistical property is the waiting-time distribution (WTD), that is the distribution of times between individual type III events within the storm. WTD analysis has been applied to soft X-ray flares (Wheatland 2000; Wheatland & Litvinenko 2002) and coronal mass ejections (Wheatland 2003), and in both cases it has been shown that the data are consistent with a time-dependent Poisson process, in which events occur independently. The WTD provides models with extra constraints; for example, flare avalanche models (e.g., Lu et al. 1993) predict that flares occur independently, and so the WTD is an important observable.

To our knowledge, the WTD has not been used to examine type III storms, particularly at the low radio frequencies typically measured by spacecraft (below ∼16 MHz). In this Letter, we analyze both the brightness distribution and the WTD of a type III storm observed by the S/WAVES radio experiment
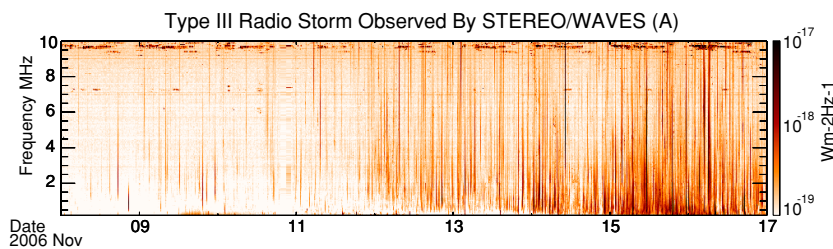
Figure 1. STEREO/WAVES (A) observations of radio emission from 2006 November 8 0000 UT to 2006 November 17 0000 UT (9 days). A type III storm associated with AR 10923 was observed, beginning on November 11. Terrestrial RFI is observed periodically between 9.5 MHz and 10 MHz but is avoided in the analysis. The white line at 2 MHz is an artifact of the plotting software.

(Bougeret et al. 2008) on board the STEREO spacecraft (Kaiser et al. 2008), in order to examine in more detail the underlying processes responsible for type III storm emission.

2. OBSERVATIONS

Each STEREO spacecraft is equipped with an identical S/WAVES instrument designed to measure both in situ plasma waves and freely propagating radio emission in the frequency range from 2.5 kHz to 16.025 MHz (Bougeret et al. 2008). S/WAVES uses three orthogonal monopole electric antennas (Bale et al. 2008) connected to two instrument channels; in a typical operating mode, one channel is connected to a pseudodipole and the other to a monopole. Within each channel, there is a high-frequency receiver (HFR) and a low-frequency receiver (LFR). The observations presented here were obtained shortly after launch using the HFR which covers the frequency range from 125 kHz to 16.025 MHz, before the lunar flybys that sent the STEREO spacecraft into their final heliocentric orbits and before many of the other instruments became operational. Consequently, the radio data from the two spacecraft are essentially identical, and so here we present the analysis from STEREO A.

Figure 1 shows measurements from the S/WAVES experiment on STEREO A measured between 0.2 MHz and 10 MHz from 2006 November 8 0000 UT–2006 November 17 0000 UT; 9 days of data are shown. The data are from channel 1 (corresponding to the $E_x - E_y$ dipole), and have been calibrated in units of incident flux S (W m^{-2} Hz^{-1}) following the procedure described by Eastwood et al. (2009). The calibration procedure is most accurate below ~10 MHz; at higher frequencies, the antenna resonance is less well modeled. Lines of radio frequency interference (RFI) at fixed frequencies have been removed by averaging across the frequency band. Terrestrial RFI is still observed periodically between 9.5 MHz and 10 MHz; in the following analysis, frequencies have been chosen to avoid this interference.

Type III emission began to be observed intermittently as early as 2006 November 9, and the storm itself was established by 2006 November 11. Active region (AR) 10923 was the only active region on the disk during this time, so we associate it with the type III storm (Kayser et al. 1987) although it appears that the storm developed after the active region appeared on the disk. Over the next 6 days, the number, frequency, and intensity of type III emissions increased. On November 17, the STEREO spacecraft executed an Earth perigee pass. While the storm continued, S/WAVES observed overwhelming terrestrial RFI at all frequencies. Active region 10923 was close to the limb by this time, and a drop in the number and intensity of type III bursts on November 18 was followed by the leading spot of AR 10923 rotating past the limb on November 20. This

confirmed the association of the active region with the type III bursts (Bougeret et al. 1984b), but suggests that the activity is more associated with the leading edge of the region. In this Letter, the interval between 2006 November 11 0000 UT and 2006 November 17 0000 UT has been analyzed.

3. ANALYSIS AND RESULTS

To examine the properties of this storm interval in more detail, time series of data at specific frequencies were extracted and analyzed. Identification of individual type III bursts was made in the following way. We first established a threshold brightness S_0 and defined a burst as an interval during which time the brightness S satisfies $S > S_0$. The burst was then assigned a brightness $S_{burst} = S_{max} - S_g$, the maximum brightness during the burst interval minus the galaxy brightness S_g (Cane 1979). The time of the burst is similarly defined as the time the maximum brightness was observed. Inspection of the data during the most active intervals shows that in general, bursts are typically observed to last only one time step (~25 s), and bursts lasting multiple time steps are rare. Accordingly, mis-counting from event overlap is not significant. This results in a set of N bursts and from their observed times, a set of $N - 1$ waiting times.

We first consider the brightness distribution $f(S)$, which we define as the number of bursts per unit brightness. If this distribution follows a power law

$$f(S) = A S^{-\delta}, \qquad (1)$$

then the maximum likelihood method (Bai 1993) can be used to show that the most likely value of the power-law index δ_m is given by

$$\delta_m = \frac{N}{\sum_{i=1}^{N} \ln(S_i/S_0)} + 1, \qquad (2)$$

where S_i is the brightness of the ith burst. The error associated with δ_m is given by Wheatland (2004):

$$\sigma_\delta \sim (\delta_m - 1) N^{-1/2}. \qquad (3)$$

Rather than examining the brightness distribution directly, it is preferable to plot the cumulative brightness distribution, which avoids binning of the data, and more easily shows the effect of the choice of S_0. The cumulative distribution also follows a power law as shown by Equation (4):

$$N_{S>S_0} = \int_{S_0}^{\infty} A S^{-\delta} dS = \frac{A}{\delta - 1} S_0^{-\delta+1}. \qquad (4)$$

This analysis was applied to the 3.025 MHz time series. Figure 2 shows the distribution of cumulative burst brightness
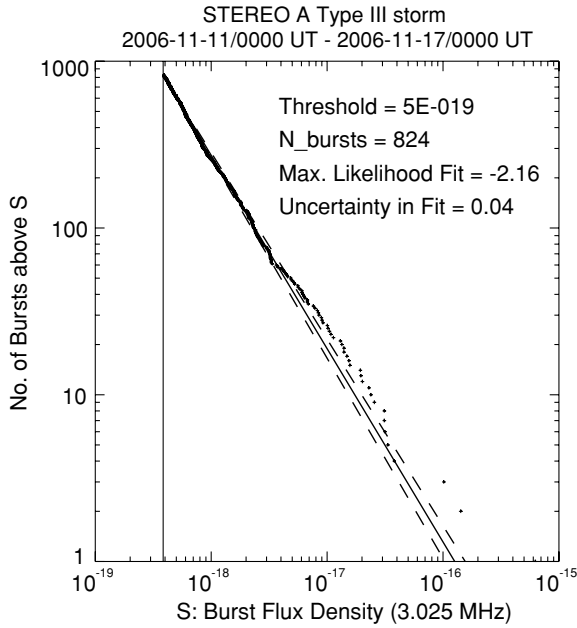
STEREO A Type III storm
2006-11-11/0000 UT - 2006-11-17/0000 UT

Threshold = 5E-019
N_bursts = 824
Max. Likelihood Fit = -2.16
Uncertainty in Fit = 0.04

Figure 2. Cumulative distribution of burst brightness at 3.025 MHz, together with the maximum likelihood fit.

Table 1
Power-law Index as a Function of Frequency

Frequency (MHz)	Power-law Index
3.025	2.16 ± 0.04
4.025	2.13 ± 0.04
5.025	2.10 ± 0.05
6.025	2.15 ± 0.06
7.025	2.24 ± 0.06
8.025	2.22 ± 0.07
9.025	2.36 ± 0.07
10.025	2.20 ± 0.07

(points). A threshold $S_0 = 5 \times 10^{-19}$ W m^{-2} Hz^{-1} is used, well above the average galactic brightness of $\sim 1.1 \times 10^{-19}$ W m^{-2} Hz^{-1}. This results in a set of 824 bursts. In this case, the power-law index associated with the brightness distribution is $\delta = 2.16 \pm 0.04$. The power law derived from the data using the maximum likelihood method is shown as a solid line in Figure 2; dashed lines show the power law plus/minus the error calculated using Equation (3). The data in general follow the power law, and the significance of any departure in the final few points is marginal; there is no substantial evidence for a break to a different power-law index although a detailed quantitative model comparison has not been done. If a higher value of S_0 is chosen, this has the effect of removing points on the left-hand side of the cumulative distribution, but does not change the index of the power law. If a smaller value of S_0 is chosen, the data eventually roll over to the background level. This procedure was repeated for other frequencies and the results are shown in Table 1. It can be seen that there is very little variation in the power-law index as the frequency changes. A larger power-law index is seen compared to the study of type III bursts (Fitzenreiter et al. 1976).

The top panel of Figure 3 shows the time series at 3.025 MHz, where the horizontal line indicates the threshold used in the analysis. The middle panel of Figure 3 shows the cumulative number of bursts as a function of time. It can be seen that the number of bursts does not increase at a constant rate, rather
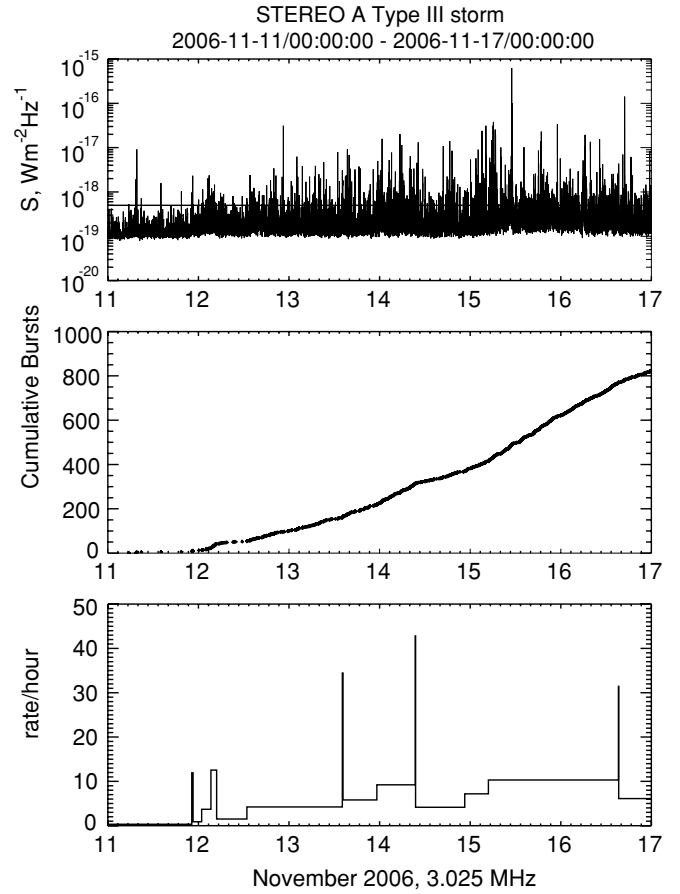
STEREO A Type III storm
2006-11-11/00:00:00 - 2006-11-17/00:00:00

Figure 3. Top: time series at 3.025 MHz; middle panel: cumulative number of bursts; and bottom panel: results of the Bayesian blocks decomposition.

there are intervals where the number of bursts increases slowly, followed by shorter intervals where the burst rate is enhanced, and the cumulative number of bursts increases more rapidly. To quantify this, a Bayesian block procedure (Scargle 1998; Wheatland 2000) was used to decompose the data into intervals consistent with a constant-rate Poisson process. Since a Poisson process has a WTD given by

$$P(\Delta t) = \lambda e^{-\lambda \Delta t}, \qquad (5)$$

where Δt is the interval between events and λ is the rate, a piecewise-constant Poisson process made up of M intervals with rates λ_i and durations t_i has a WTD given by

$$P(\Delta t) \approx \frac{1}{\bar{\lambda}} \sum_{i=1}^{M} \frac{t_i}{T} \lambda_i^2 e^{-\lambda_i \Delta t}, \qquad (6)$$

where $\bar{\lambda}$ is the average burst rate and T is the duration of the observing interval (e.g., Wheatland & Litvinenko 2002). The bottom panel of Figure 3 shows the Bayesian blocks rate decomposition. The Bayesian procedure decided that there were $M = 16$ intervals with approximately constant rate during the observing period.

The top panel of Figure 4 shows the observed WTD as points. The data are again presented cumulatively to avoid binning of the data. The model cumulative WTD is given by

$$P(\Delta t > \Delta t_0) = \int_{\Delta t_0}^{\infty} P(\Delta t) d\Delta t \approx \frac{1}{\bar{\lambda}} \sum_i \frac{t_i}{T} \lambda_i e^{-\lambda_i \Delta t_0}, \qquad (7)$$

where the rates λ_i and intervals t_i come from the Bayesian blocks

STEREO A Type III storm
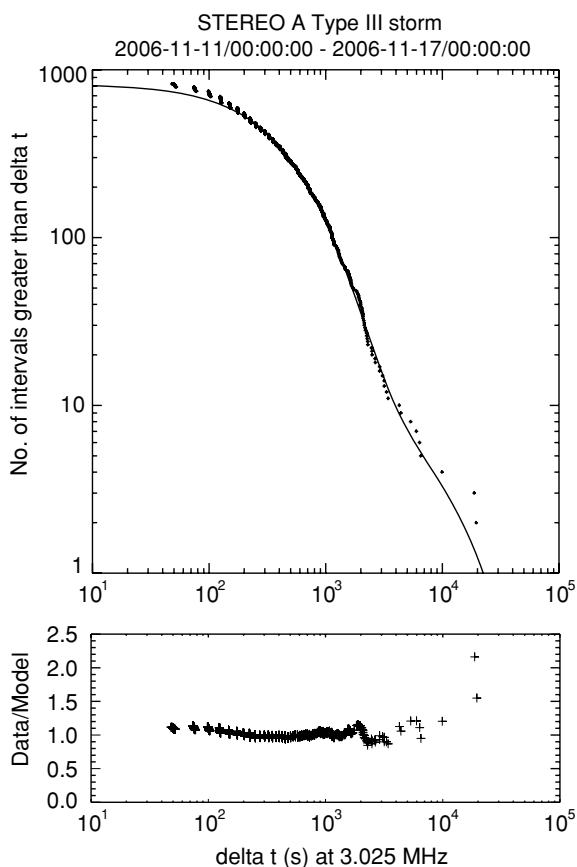2006-11-11/00:00:00 - 2006-11-17/00:00:00

Figure 4. Top panel shows the cumulative WTD of bursts at 3.025 MHz, together with model based on a piecewise constant Poisson process, with rates determined by the Bayesian blocks procedure. The bottom panel shows the ratio of the data and the model.

procedure. This model is also shown in the top panel of Figure 4. The bottom panel of Figure 4 shows the ratio of the data and the model as a function of waiting time. There is good agreement between the data and the model, which strongly suggests that the observed WTD is consistent with a piecewise-constant Poisson process whose rate varies as shown in Figure 3. Similar results were obtained for the different frequencies shown in Table 1.

4. DISCUSSION

As mentioned in the introduction, type III emission is thought to arise from nonthermal electron beams on open field lines. Emission may occur at the fundamental or its harmonic; type III bursts whose trajectory intersects the spacecraft show that the emission is at the fundamental mode (Leblanc et al. 1998; Dulk 2000), but the possibility of harmonic emission perhaps should not be discounted (Kellogg 1980; Bougeret et al. 1984b). Since the local electron plasma frequency depends on density (that is, $f_p(\text{Hz}) = 8.98 \times 10^3 \times (n_e(\text{cm}^{-3}))^{1/2}$) a density model is required to determine the height of the radio emission. Using the model developed by Leblanc et al. (1998), in this example 2 MHz corresponds to $\sim 3\,R_S$ and 9 MHz corresponds to $\sim 1.8\,R_S$. The model is scaled to the solar wind density at 1 AU; between 2006 November 17 and 20 the average solar wind density measured by the *Advanced Composition Explorer* spacecraft at 1 AU is approximately 4 cm^{-3}. If the type III emission is harmonic, then the local density is reduced, and the emission comes from higher in the corona—between approximately 2.5 and 9 R_S for 9 MHz and 2 MHz.

It is generally accepted that the radio emission arises from the nonlinear conversion of Langmuir waves excited at the local plasma frequency by nonthermal electron beams. As the electrons move along the magnetic field, the faster electrons outrun the slower electrons leading to a bump-on-tail distribution and instability (Robinson & Cairns 2000). The growth of Langmuir waves causes the distribution to relax to marginal stability; in stochastic growth theory, fluctuations in the ambient density are thought to cause fluctuations about marginal stability which allows wave growth without rapid destruction of the electron beam (Robinson 1992; Robinson et al. 1993). This suggests that the electron beams are being emitted from closer to the Sun. The more general association of type III storms (open field) and type I storms (closed field) suggests that the storm activity is related to reconfiguration of the boundary between open and closed magnetic fields in the underlying active region. Analysis of potential field source surface maps (Schrijver & DeRosa 2003) shows that a small region of open field lines was persistently present adjacent and to the west of the active region during the storm. The interface between the open and closed field regions rotated behind the limb before the active region itself, which may help to explain the observed decline in storm activity prior to the active region rotating past the limb.

In this type III storm, a $S^{-2.1}$ power law was found in the number distribution, corresponding to a $S^{-3.1}$ power law in the number/unit flux density. The power-law index was found to be largely independent of frequency. Although the exact relationship between the primary energy release, the energy and properties of the electron beam, and the energy converted to radio emission is not well understood, it is likely that this reflects power-law behavior in the underlying dynamics. In a previous study, Morioka et al. (2007) observed a $S^{-3.6}$ power law in the number distribution of the storm ("micro") burst population, but this was averaged over several storm intervals and used data binning. In this analysis, maximum likelihood was used, although this technique should be used with care if there are departures from the power-law behavior due to the method of event selection, background subtraction, etc. It is necessary to study other events to understand whether this difference represents variability from storm to storm, or is due to some other effect. The rate at which bursts are observed is found to change through the storm. Using a Bayesian block decomposition, we find the observed WTD to be consistent with a piecewise-constant Poisson process, which indicates that individual type III bursts occur independently of one another. It is interesting to note that the Bayesian block structure has no correlation with the occurrence of flares in the active region. A GOES C3.3 event occurred on 2009 November 12 at 2155 UT, for example, in the middle of a long Bayesian block.

These two properties are predicted by avalanche models of driven systems. In the solar context, such models have been developed to understand the properties of solar flares (Lu et al. 1993). This suggests that in the active region under consideration, magnetic energy and flux, slowly injected from below and being driven e.g., by twisting due to footpoint motion, are being released in a series of independent events which result in the emission of electron beams onto open field lines. In particular, the long lifetime of type III storms indicates that the active region can remain in such a dynamically balanced state for a prolonged period of time even as the burst rate slowly changes. This stability was not disturbed by the ~ 21 GOES flares in this time interval from AR 10923, including five C-class events before 2006 November 14.

Facilities: STEREO

REFERENCES

Bai, T. 1993, ApJ, 404, 805
Bale, S. D., et al. 2008, Space Sci. Rev., 136, 529
Bougeret, J.-L., Fainberg, J., & Stone, R. G. 1984a, A&A, 136, 255
Bougeret, J.-L., Fainberg, J., & Stone, R. G. 1984b, A&A, 141, 17
Bougeret, J.-L., et al. 2008, Space Sci. Rev., 136, 487
Cane, H. V. 1979, MNRAS, 189, 465
Dulk, G. A. 2000, Radio Astronomy at Long Wavelengths Geophysical Monograph, Vol. 119 (Washington, DC: AGU), 115
Eastwood, J. P., Bale, S. D., Maksimovic, M., Zouganelis, I., Goetz, K., Kaiser, M. L., & Bougeret, J.-L. 2009, Radio Sci., 44, RS4012
Fainberg, J., & Stone, R. G. 1970a, Sol. Phys., 15, 222
Fainberg, J., & Stone, R. G. 1970b, Sol. Phys., 15, 433
Fainberg, J., & Stone, R. G. 1971, Sol. Phys., 17, 392
Fitzenreiter, R. J., Fainberg, J., & Bundy, R. B. 1976, Sol. Phys., 46, 465
Gopalswamy, N. 2004, Planet. Space Sci., 52, 1399
Kaiser, M. L., Kucera, T. A., Davila, J. M., St. Cyr, O. C., Guhathakurta, M., & Christian, E. 2008, Space Sci. Rev., 136, 5
Kayser, S. E., Bougeret, J.-L., Fainberg, J., & Stone, R. G. 1987, Sol. Phys., 109, 107
Kellogg, P. 1980, ApJ, 236, 696
Leblanc, Y., Dulk, G. A., & Bougeret, J.-L. 1998, Sol. Phys., 183, 165
Lu, E. T., Hamilton, R. J., McTiernan, J. M., & Bromund, K. R. 1993, ApJ, 412, 841
Mercier, C., & Trottet, G. 1997, ApJ, 474, L65
Morioka, A., Miyoshi, Y., Masuda, S., Tsuchiya, F., Misawa, H., Matsumoto, H., Hashimoto, K., & Oya, H. 2007, ApJ, 657, 567
Reiner, M., Kaiser, M. L., Karlicky, M., Jiricka, K., & Bougeret, J.-L. 2001, Sol. Phys., 204, 123
Robinson, P. A. 1992, Sol. Phys., 139, 147
Robinson, P. A, Cairns, I. H., & Gurnett, D. A. 1993, ApJ, 407, 790
Robinson, P. A., & Cairns, I. H. 2000, Radio Astronomy at Long Wavelengths Geophysical Monograph, Vol. 119 (Washington, DC: AGU), 37
Scargle, J. 1998, ApJ, 504, 405
Schrijver, C. J., & DeRosa, M. L. 2003, Sol. Phys., 212, 165
Wheatland, M. S. 2000, ApJ, 536, L109
Wheatland, M. S. 2003, Sol. Phys., 214, 361
Wheatland, M. S. 2004, ApJ, 609, 1134
Wheatland, M. S., & Litvinenko, Y. E. 2002, Sol. Phys., 211, 255